Journal of Operational Meteorology
Article

Choosing a Universal Mean Wind for Supercell Motion Prediction

MATTHEW J. BUNKERS *and* DAVID A. BARBER
NOAA/NWS Forecast Office, Rapid City, South Dakota

RICHARD L. THOMPSON, ROGER EDWARDS, *and* JONATHAN GARNER
NOAA/NWS/NCEP/Storm Prediction Center, Norman, Oklahoma

ABSTRACT

The 0–6-km AGL mean wind has been used widely in operations to predict supercell motion. However, when a supercell is low-topped or elevated, its motion may be poorly predicted with this default mean wind—which itself could be height-based or pressure-weighted. This information suggests that a single, fixed layer is inappropriate for some situations, and thus various mean-wind parameters are explored herein.

A dataset of 583 observed and 829 Rapid Update Cycle supercell soundings was assembled. When the mean wind is computed using pressure weighting for an effective inflow-layer as the base, and 65% of the most-unstable equilibrium level height as the top, the result is that better supercell motion predictions can be obtained for low-topped and elevated supercells. Such a mean-wind modification would come at the cost of only a minor increase in mean absolute error for the entire sample of supercell cases considered.

1. Introduction

Despite advances in our understanding of the prediction of supercell motion, considerable challenges remain. Perhaps most importantly, predictions as of this writing rely mainly on the hodograph, and thus, outside of effective-inflow parcels (Thompson et al. 2007, hereafter T07), ignore potentially relevant thermodynamic information. At times this omission can lead to large forecast errors. For example, subcloud relative humidity and the lifted condensation level (LCL) may be germane in modulating the downshear movement of storms (Kirkpatrick et al. 2007). Another pertinent consideration (not addressed here) is atmospheric boundaries; in situations with large buoyancy and/or relatively weak shear, boundaries may substantially change the motion of storms from what is anticipated (e.g., Weaver 1979; Atkins et al. 1999; Zeitler and Bunkers 2005). Even sophisticated convection-allowing models can have difficulty in predicting supercell motion and location for lead times >1–2 h (Cintineo and Stensrud 2013).

One area of potential improvement in supercell motion prediction involves the selection of the mean wind, which represents the advective component of supercell motion. To date, most algorithms rely on a fixed layer (e.g., Maddox 1976; Davies and Johns 1993; Bunkers et al. 2000, hereafter B2K). Rasmussen and Blanchard (1998) did not specify a mean wind per se, but their method implicitly uses (i) the surface as the lower bound for the mean wind and (ii) a percentage of the shear vector as a proxy for the mean-wind depth. In general, the 0–6-km layer is the default when predicting supercell motion (e.g., Weisman and Klemp 1986; Davies and Johns 1993; B2K), although other studies have included mandatory sounding data up to levels in the 300–200-hPa range (e.g., Newton and Fankhauser 1964; Maddox 1976; Chappell 1986, pp. 292–296). Ramsay and Doswell (2005, hereafter RD05) evaluated several supercell-motion prediction methods and suggested that the height-based mean wind for the 0–8-km layer was most appropriate, on average; this was a proposed increase to B2K's 0–6-km layer. RD05 also considered variations in the mean-wind depth as a function of the LCL, level of free convection (LFC), and equilibrium level (EL), but they discovered no improvement in supercell motion predictions.

Corresponding author address: Dr. Matthew J. Bunkers, National Weather Service, 300 E. Signal Dr., Rapid City, SD 57701
E-mail: matthew.bunkers@noaa.gov

After these studies, T07 evaluated a mean-wind layer constrained by buoyancy and convective inhibition and found mixed results—favorable for elevated supercells (defined below) but no improvement noted for typical supercells (i.e., those with tops around 12 km AGL; Moller et al. 1994). Specifically, T07 (p. 107) noted that "The original ID [B2K] method resulted in the smallest mean absolute error (4.6 m s^{-1}), our two ID modifications scaled to storm depth both produced mean absolute errors near 4.8 m s^{-1}, and the RD05 modification to the ID method resulted in the largest mean absolute error (4.9 m s^{-1})."

Another possible modification to the mean wind applies to low-topped, miniature, or "shallow" supercells (e.g., Davies 1990, 1993). Arguably these are less common than the prototypical Great Plains supercell, except in tropical cyclones (e.g., McCaul and Weisman 1996; Spratt et al. 1997; Rao et al. 2005; Edwards et al. 2012). Still, they can produce substantial severe weather, including tornadoes (e.g., Grant and Prentice 1996; McCaul and Weisman 1996; Wicker and Cantrell 1996; Jungbluth 2002; Darbe and Medlin 2005; Graham 2007; Richter 2007; among others). This class of supercells usually has a below-average storm top, and thus should move with a mean wind over a relatively shallower layer than the typical supercell. Nevertheless, Spratt et al. (1997, their Fig. 4) provided an example of a "low-topped" storm in which the EL was near 14 km AGL.

As alluded to above, the storm-inflow layer also helps to regulate the mean wind. Surface-based supercells (e.g., Corfidi et al. 2008) thus should have the base of the mean-wind computation layer at the ground. Accordingly, RD05 noted that the B2K scheme had the most accurate forecasts for a mean-wind layer that originated below the LCL, near the surface. This finding is consistent with our observed dataset, whereby most of the soundings were collected around the time of peak surface heating and vertical mixing (refer to section 2a below)—when the probability of elevated supercells is at a relative minimum.

Some other supercells derive a part of their inflow from above the surface, and these are referred to as elevated supercells (e.g., Grant 1995; Calianese et al. 1996; Corfidi et al. 2008). Accordingly, the air near the ground may have little relevance to forecasting the motion of these storms, but not necessarily in all cases (Nowotarski et al 2011). How to define an elevated supercell is thus problematic, because no long-established criteria exist to define the base of the storm-inflow layer. T07 briefly discussed concerns about the use of the most-unstable (MU) parcel height compared to the effective inflow-layer base (EffB) for this purpose. The EffB is defined as the lowest level where parcels possess non-negligible buoyancy without excessive inhibition. An EffB *above the ground* is a fairly stringent criterion for an elevated supercell, requiring surface lifted parcel buoyancy <100 J kg^{-1} or surface-based convective inhibition (CIN) >250 J kg^{-1}. An MU parcel height above the ground is a less stringent criterion, compared to the EffB technique. Relying on the EffB technique, T07 found for a small subset of 16 elevated supercells that the mean absolute error (MAE) using the B2K method was reduced by about 2 m s^{-1} when disregarding the surface-based stable layer.

In one of the few modeling studies of storm motion, Kirkpatrick et al. (2007) noted that the LCL and LFC had the most pronounced thermodynamic control on storm motion. They further suggested that the appropriate mean-wind layer may extend from the surface to a height that is a function of the LFC. However, the LFC is more spatially related to the base of the mean wind rather than the top of the mean wind. Accordingly, the height of the MU parcel, as well as the height of the EffB, can be used in lieu of the LFC to evaluate whether an above-surface level is appropriate as the base of the mean wind.
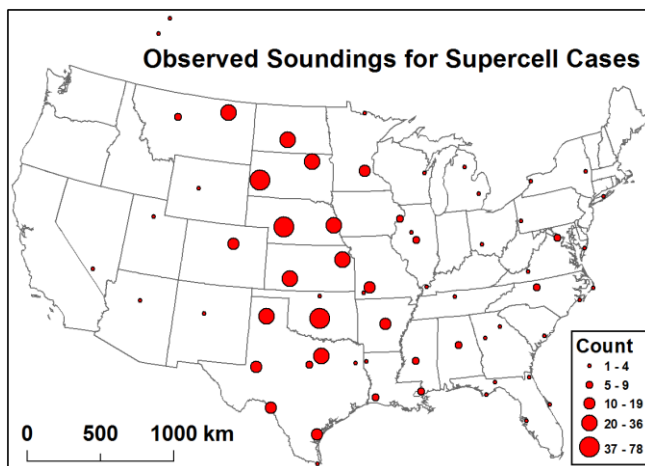
In addition to the mean-wind options just reviewed, sometimes lost in the calculation of the mean wind is the weighting—often done by pressure—of the individual wind levels that contribute to the calculation. Yet, it is unclear if the height-based mean wind is consistently superior to the pressure-weighted mean wind for supercell motion. These mean-wind options and weightings can result in nontrivial differences in the mean wind. Therefore, in light of these variations in (i) supercell bases and tops, (ii) proposed layers for the mean wind, and (iii) pressure-weighting options, the purpose of this article is to determine if a universal method of calculating the mean wind can be used in the prediction of supercell motion. Our goal is to minimize the overall errors in a way to make the method effective in all environments.

2. Data and methods

a. Supercells and soundings

The observational supercell datasets from Bunkers (2002) and Bunkers et al. (2006) were used for this study. Using their methods, 302 additional cases were randomly collected from 2006 to 2013, and these were

used to augment the dataset. Supercell identification was based on a combination of radar reflectivity (e.g., hook echoes, midlevel overhang, inflow gradients, and storm steadiness) and velocity (i.e., a persistent and deep azimuthal velocity difference of ≥20 m s^{-1}). A total of 615 observed cases subsequently was assembled for this work. Because storm sub-classification was an ancillary focus at that time, little attempt was made to discriminate among low-topped, elevated, or typical supercells. However, based on the geographic and temporal attributes of the database, we estimated that >80% of the cases comprise typical supercells. Consistent with this claim, 88% of the cases occurred from April to September, and 82% were gathered from the central United States—east of the Rocky Mountains and west of the Mississippi River (Fig. 1). There is a bias of cases across the northern high plains where initial data collection was more strongly focused (B2K), and thus Fig.1 does not constitute a climatology.

Figure 1. Sounding locations for the 615 observed cases with kinematic-only data. Symbol size is proportional to the number of cases per sounding location (min = 1 and max = 78). One case is from Hawaii (not shown), two cases are from Canada, and the rest are from the contiguous United States. The projection is North America Lambert conformal conic. *Click image for an external version; this applies to all figures hereafter.*

Soundings for the observed cases (obtained from esrl.noaa.gov/raobs/) represent the inflow region of the supercells, and supercells generally occurred within 3 h and 185 km (100 n mi) of the sounding release. Soundings were discarded if a subjective assessment found that they were likely to be contaminated by convection (as in Bunkers et al. 2006). Ninety percent of the cases are associated with a 0000 UTC release; 4% are associated with a 1200 UTC release; and the remaining 6% are associated with 1800–2100 UTC

releases. The observed supercell motion was calculated during the most isolated and/or steadiest part of the supercell's low-level radar reflectivity echo using a duration of around 60 min. Furthermore, each case consists of a single, observed, unmodified sounding so as to avoid assumptions and potential problems associated with (i) subjective modifications and (ii) interpolating between observations.

All parcel-related calculations used the virtual temperature correction (Doswell and Rasmussen 1994; also see www.flame.org/~cdoswell/virtual/virtual.html). The MU parcel was found by determining the largest value of equivalent potential temperature in the lowest 350 hPa of the sounding, and the mean-layer (ML) parcel was calculated by averaging potential temperature and mixing ratio in the lowest 1 km of the sounding[1]. The EffB was calculated as in T07 (i.e., the first level where CAPE ≥100 J kg^{-1} and CIN ≤250 J kg^{-1}). Soundings with MUCAPE <50 J kg^{-1}, or a missing or zero MUEL[2], were discarded. This constraint reduced the useable observed dataset with *concurrent* kinematic and thermodynamic information to 583 cases (a 5% reduction from the total); however, 615 cases were available for kinematic-only calculations.

In addition to the 583 observed cases, a second dataset of 833 supercell cases with corresponding Rapid Update Cycle (RUC) 0-h forecast soundings was obtained from T07 (see their Fig. 1 for the geographical distribution). This dataset spans from April 1999 to March 2005. These RUC soundings were interpolated from a 40-km grid to the nearest surface-observation location, and were within 40 km and 30 min of radar-identified discrete supercells; T07 have additional details on the interpolations. Given the cool and dry biases in the RUC surface fields reported by Thompson et al. (2003), these 0-h RUC soundings were modified with the nearest surface observation for temperature and dewpoint. The surface observations were manually inspected for each case to avoid (i) unrepresentative surface observations and (ii) mismatches between surface observations and RUC soundings.

---

[1] Although the Storm Prediction Center uses the lowest 100 hPa for the ML parcel, the lowest 1 km is used herein based on the work of Rasmussen and Blanchard (1998). The two layers are not identical, but to a first-order approximation 10 m corresponds to 1 hPa in the lower troposphere. Hence, the lowest 1 km of the atmosphere is about 100 hPa deep (to within 5–10%).

[2] The MUEL was chosen instead of the MLEL based on results from T07. Moreover, the MLEL was tested for the present study, but MAEs were 0.17 m s^{-1} larger relative to those for the MUEL.

Non-surface model sounding levels were left unmodi-fied owing to a paucity of real-time observational data above the ground in the majority of cases. Like for the observed cases, these RUC cases were not sub-classi-fied into low-topped, elevated, or typical supercells. The final RUC dataset consists of 829 cases owing to the MUCAPE and MUEL constraints noted above.

b. Mean-wind calculations

The mean wind was calculated with respect to height by interpolating the *u*- and *v*-components to a 500-m spaced vertical grid from the surface to 12 km AGL. Next, the components were summed over the relevant levels, *N* (e.g., *N* = 13 for the 0–6-km mean wind), and then divided by *N*, as follows:

$$\bar{u} = \frac{\sum_1^N u_i}{N}, \tag{1a}$$

$$\bar{v} = \frac{\sum_1^N v_i}{N}, \tag{1b}$$

where $i = 1, 2, \ldots, N$. The pressure-weighted mean wind was calculated analogous to Eq. (1), but with a weighting term as follows:

$$\bar{u} = \frac{\sum_1^N u_i \times \left(\frac{p_i}{\bar{p}}\right)}{N}, \tag{2a}$$

$$\bar{v} = \frac{\sum_1^N v_i \times \left(\frac{p_i}{\bar{p}}\right)}{N}, \tag{2b}$$

where p is the pressure at a given level, i, and $\bar{p}$ is the simple average pressure for the layer from 1 to N (using all gridded pressure values every 500 m). In the lower half of the layer the weights are mostly ≥1 and in the upper half they are mostly ≤1 (e.g., Fig. 2, light gray line for a 0–12-km layer). Additionally, other pressure-weighting options were explored as follows:

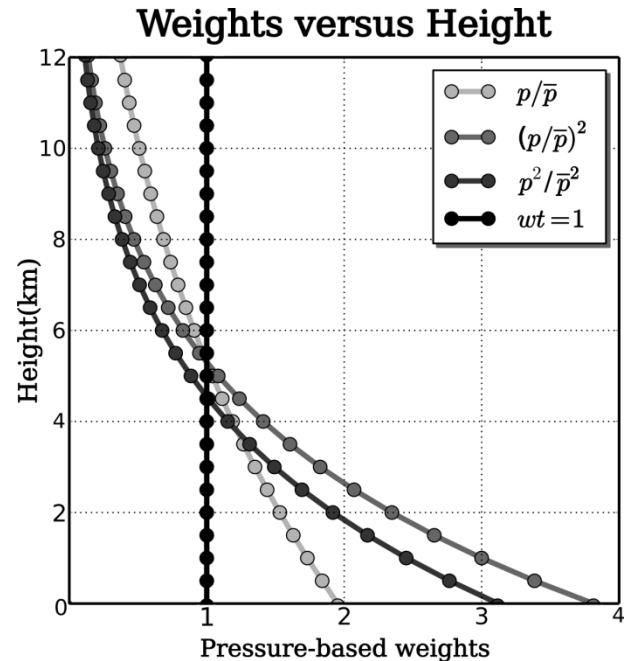$$\bar{u} = \frac{\sum_1^N u_i \times \left(\frac{p_i}{\bar{p}}\right)^2}{N}, \tag{3a}$$

$$\bar{v} = \frac{\sum_1^N v_i \times \left(\frac{p_i}{\bar{p}}\right)^2}{N}, \tag{3b}$$

and

$$\bar{u} = \frac{\sum_1^N u_i \times \left(\frac{p_i^2}{\bar{p}^2}\right)}{N}, \tag{4a}$$

$$\bar{v} = \frac{\sum_1^N v_i \times \left(\frac{p_i^2}{\bar{p}^2}\right)}{N}. \tag{4b}$$

Recall that the mean wind with respect to height gives equal weighting in space over the mean-wind layer (Fig. 2, black vertical line). Conversely, pressure weighting [e.g., Eq. (2)] gives relatively more weight to the lower atmosphere versus the upper atmosphere. Equations (3)–(4) go even further by weighting the lower atmosphere at about double that of Eq. (2), and weight the upper atmosphere at about two-thirds of Eq. (2). The 0–12-km layer weights in Fig. 2 are qualita-tively similar to the weights for a shallower layer, but as the layer depth decreases the range of the weights also decreases (e.g., about 0.7–1.4 for the 0–6-km lay-er); the weights approach unity for a very thin layer. These pressure-weighting equations were employed to ascertain just how much influence the lower atmo-sphere should be given to the mean-wind calculation for supercell motion.

Figure 2. An example of weights for the pressure-based mean-wind options employed in this study (for a 0–12-km layer). The light gray line [Eq. (2)] is the commonly used method, whereas the moderate gray line [Eq. (3)] and the dark gray line [Eq. (4)] repre-sent variations to pressure weighting. The height-based method [vertical black line, Eq. (1)] is plotted for reference; weights = 1 are inferred in Eq. (1).

Finally, after considering the work of T07, the top of the mean-wind layer was investigated as a function of the MUEL depth—in addition to fixed heights AGL. To do this step, the top was varied from 10% of the MUEL to 100% of the MUEL at 5% increments. Additionally, the base of the mean-wind layer was constrained to be one of the following: (i) surface, (ii) height of the MU parcel, or (iii) height of the EffB. Combinations of these settings were explored to determine the best-performing method; the MAE was used for this purpose, and calculated as the magnitude of the vector difference between the observed and predicted motion vectors.

3. Results and discussion

a. Potential improvements in supercell motion prediction: Observed dataset

Early in this work a sensitivity test was conducted to assess the potential improvements of tuning the parameters of the B2K method (i.e., mean wind and deviation from the mean wind) to predict supercell motion. Using the 615 observed cases with kinematic data, the mean-wind layer was varied from 0–3- to 0–12-km at 1-km increments (i.e., ten layers per case); the wind-shear layer as prescribed in B2K was held constant. Improvements of 1.31 m s^{-1} MAE are possible under this scenario *if the best choice for the mean-wind layer is made a priori*. Harnessing this potential would be an operationally significant improvement, and is 0.26 m s^{-1} larger than the potential improvement for the deviation parameter (1.05 m s^{-1}; Bunkers 2006). Thus, the mean wind was chosen for further investigation given its slightly greater potential improvement over the deviation from the mean wind. Furthermore, Bunkers and Zeitler (2000) and Bunkers (2006) already investigated potential improvements for the deviation parameter, and reported inconclusive results. Even if both of these potential improvements (i.e., mean wind and deviation from the mean wind) could be fully realized, a residual supercell motion error of about 2 m s^{-1} would remain, mostly attributable to external effects (e.g., boundaries, mergers, and interactions with topography).

b. Mean-wind settings that minimize the MAE for supercell motion prediction: Observed dataset

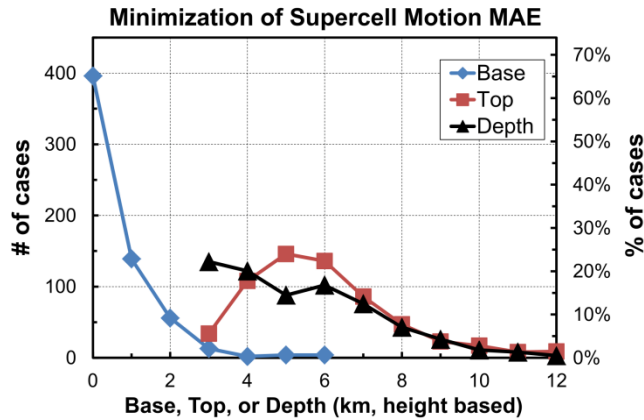In a preliminary attempt to determine what mean-wind settings (i.e., base, top, and depth) minimize the MAE in supercell motion, the 615 observed cases with kinematic data were used to compute the forecast supercell motion, using the B2K method, for a variety of mean-wind layers (with respect to height). Accordingly, a series of iterations was performed where (i) the base of the mean wind was varied from 0 to 6 km, (ii) the top of the mean wind was varied from 3 to 12 km, and (iii) the depth of the mean wind was constrained to be ≥3 km. This minimum value in mean-wind depth is consistent with Wilson and Megenhardt (1997)[3]. Therefore, the mean-wind layer bases ranged from 0 to 6 km and the tops ranged from 3 to 12 km. This led to 49 calculations per sounding (or 30 135 total calculations for the entire dataset). The wind-shear layer was held constant as in section 2a.

The results evince a range of mean-wind settings that minimize the MAE, with an especially broad distribution for the depth and top—relative to the base (Fig. 3). For example, although 65% of the cases were best predicted using a surface-based mean wind (cf. RD05), the lowest MAE also was achieved for bases of 1 and 2 km for 23% and 9% of the cases, respectively. However, rarely did the upper extent of the "best" mean-wind base exceed 2 km. Moreover, there was a fairly uniform preference for mean-wind depths in the 3–6-km range, but with relative maxima at 3 and 6 km. Otherwise, the top of the mean-wind layer was concentrated from 4 to 7 km, comprising 78% of the cases. Even 7- and 8-km tops, collectively, were the best choice for 22% of the cases. Whereas the height-based 0–6-km layer has been shown previously to be superior in the aggregate, the most suitable mean-wind layer for supercell motion varies considerably on a case-to-case basis.

c. Mean wind with respect to height versus pressure weighting: Observed dataset

The results of comparing surface-based mean winds for different calculations (Fig. 4a) are consistent with some previous studies (B2K, T07), but partially inconsistent with RD05. Furthermore, the results provide additional insight into pressure-weighting options.
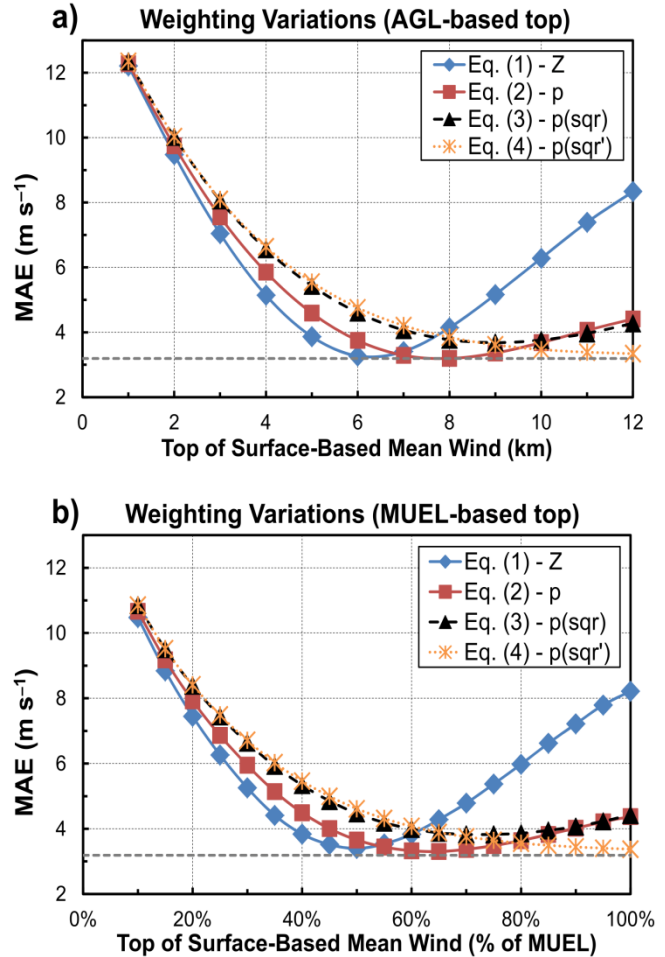
---

[3] For mean-wind depths <3 km a shallow layer artificially minimizes the MAE. The likelihood of a single level (or very shallow layer) to best predict the advective component of supercell motion—relative to a deeper layer—occurs because this level/layer can lie just about anywhere on the hodograph. However, it is unrealistic to expect a deep storm to be steered by the wind at just one or two levels, and furthermore, supercell depths rarely are <3 km.

Figure 3. Number of cases (left axis) and percent of cases (right axis) in which the base, top, or depth of the mean wind (km) produced the minimum MAE for the forecast supercell motion using the B2K method and 615 observed cases (kinematic-only data). The mean-wind calculations were done with respect to height, not pressure-weighted.

Regarding the first point, pressure weighting produced the overall minimum MAE of 3.19 m s^{-1} for the 0–8-km layer (Fig. 4a, red line). This finding is compatible with RD05 insofar as pressure weighting resulted in the overall minimum MAE, but they stated the 0–12-km layer *instead of the 0–8-km layer* resulted in the minimum MAE. When heavier pressure weighting is applied (Fig. 4a, black dashed and orange dotted lines), the surface-based mean-wind layer that minimizes the MAE becomes progressively deeper. For example, when squaring the pressure before averaging as in Eq. (4), the 0–12-km pressure-weighted mean wind results in the minimum MAE (3.34 m s^{-1}), and this MAE is only 0.15 m s^{-1} more than the minimum MAE produced when using standard pressure weighting as in Eq. (2).

With respect to height, the 0–6-km layer minimized the error at 3.27 m s^{-1} (Fig. 4a, blue line), only 0.08 m s^{-1} larger than the minimum error for the 0–8-km pressure-weighted mean wind. Again, this layer is shallower than the suggested height-based layer reported in RD05 (0–8 km), but is consistent with B2K and T07. It is difficult to reconcile these differences with RD05, but based on Fig. 4a and the additional pressure-weighting options [Eqs. (3)–(4)], RD05 conceivably applied heavier weighting in pressure than what typically is done (and what we assumed). Moreover, the height-based calculations performed by RD05 plausibly had a component of pressure weighting. This speculation is supported by the RD05 finding that their minimum median vector error was the same for both height-based and pressure-weighted calcula-

Figure 4. (a) MAE (m s^{-1}) of the forecast supercell motion for 583 observed cases that varied the mean-wind calculation by height (blue), pressure weighting (red), squared pressure weighting (black dashed), and average squared-pressure weighting (orange dotted). The dashed gray horizontal line at 3.19 m s^{-1} indicates the minimum MAE, which corresponds to the 0–8-km pressure-weighted mean wind; this minimum was valid for all combinations (i.e., weightings, bases, depths, and tops) explored within the observed dataset. The top of the mean wind was varied from 1 to 12 km AGL. (b) Same as (a) except the top of the mean wind was varied from 10 to 100% of the height of the MUEL (roughly the storm top), and the number of available observed cases was 580.

tions; furthermore, the minimum MAE for their 0–12-km pressure-weighted layer was 3.5 m s^{-1}, similar to that using Eq. (4) herein (Fig. 4a, orange dotted line).

Regardless of the differences between RD05 and the current findings, the results suggest that (i) either height-based or pressure-weighted mean winds are reasonable choices for supercell motion prediction, and (ii) a pressure-weighted mean wind requires a deeper layer of the atmosphere to minimize errors in supercell motion prediction—relative to a height-based mean wind.

d. Variations in the top and base of the mean wind: Observed and RUC datasets

1) TOP OF THE MEAN WIND

For the observed dataset, the MAE curves for the mean wind are similar whether using height AGL (Fig. 4a) or the percentage of the MUEL (Fig. 4b) as the top of the mean-wind layer. With respect to height, the MAE was minimized for 50% of the storm depth (3.40 m s^{-1}; Fig. 4b), taken here to be the surface to the MUEL. This result is in agreement with T07 who found that the 50% level was ideal for effective storm depth. For pressure weighting, the surface-to-65% of the MUEL mean wind produced an MAE of 3.30 m s^{-1} (Fig. 4b), and corresponds closely to the 0–8-km layer (cf. Fig. 4a). Finally, the MAEs for the 0–12-km (Fig. 4a) and surface-to-100% (Fig. 4b) layers also agree well.

When comparing the height-based curve to the pressure-weighted curves, the height-based curve exhibits a relatively narrow range in which the MAE was minimized (e.g., blue line, centered around 6 km in Fig. 4a). Conversely, there is a relatively broad range—above a certain height—that the pressure-weighted mean wind produced reasonable results (e.g., ≥0–7 km in Fig. 4a). The much greater slope (i.e., variance) to the MAE curve for the deeper height-based mean winds suggests there is substantial sensitivity to picking an appropriate top when using this method, whereas for pressure weighting the MAEs will remain relatively small *as long as* the mean-wind layer is sufficiently deep.

For the RUC dataset, the MAE curves (not shown) are qualitatively similar to those for the observed dataset—displaying the same attributes as noted above. Specifically, the shapes of the curves have the same pattern, with the height-based curves displaying larger MAE variance and the pressure-weighted curves having smaller MAE variance (i.e., smaller slope); distances between adjacent curves also are comparable. One minor discrepancy is that, for pressure weighting, the 0–7-km and surface-to-60% of the MUEL layers for the RUC dataset produced the minimum MAEs (slightly shallower layers than those for the observed dataset). These minimum RUC MAEs for these two layers, however, are only 0.04–0.06 m s^{-1} smaller than the RUC MAEs for the 0–8-km and surface-to-65% of the MUEL layers.

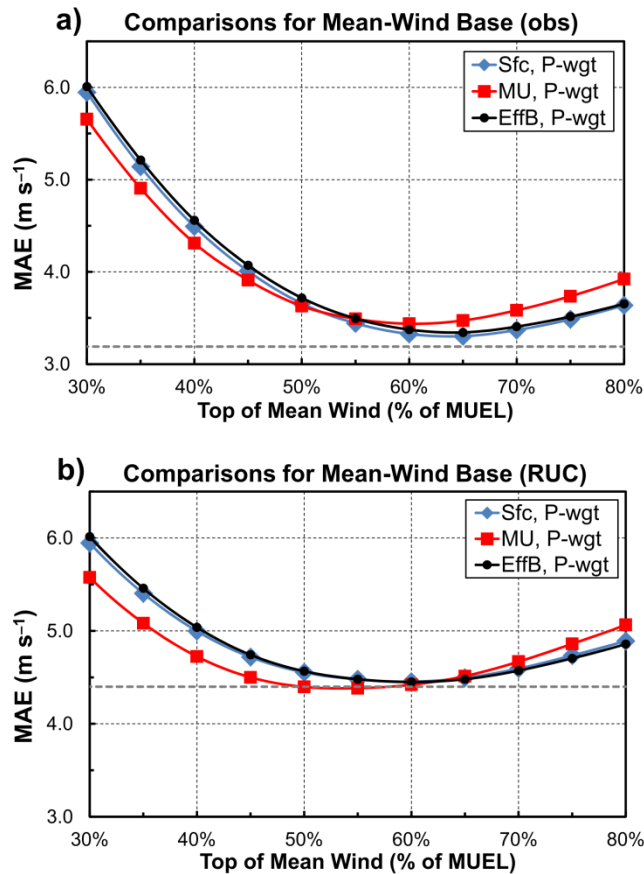Collectively, roughly half to two-thirds of the storm depth, as measured by the MUEL, is an appropriate layer for the mean wind. And even though height-based or pressure-weighted mean winds are viable options, there is a tradeoff between (i) the relatively narrow ranges of depths for an ideal height-based mean wind and (ii) pressure weighting being more computationally expensive. Moreover, variations in these mean-wind calculations can produce nontrivial differences in supercell motion, and thus forecasters should be aware of the mean wind used in operational applications.

2) BASE OF THE MEAN WIND

The results for the base of the pressure-weighted mean wind using the observed supercell dataset reveal that the errors for the surface-based and EffB mean winds are more similar to each other than to the MU-based mean wind (Fig. 5a, note the greater separation of the red line from the black and blue lines)[4]. This difference of the MU-based mean wind from the others occurs because the height of the MU parcel often is higher than the EffB height, which itself is a result of the EffB constraints for CAPE and CIN (refer to section 2a). These EffB constraints often are reached at a lower level than those of the MU parcel, making the EffB height closer to the surface; an example is given in section 3f, below. Indeed, 33% of the EffB heights had a greater pressure than that of the MU parcel heights for the observed data, but only one MU parcel height had a greater pressure than that of the EffB (all others were equal). In total, the MU parcel was above the surface for 196 (33.6%) of the observed cases, whereas the EffB was above the surface for only 36 (6.2%) of the observed cases. Finally, the minimum MAE for the MU-based mean wind occurs at a shallower depth (60%, Fig. 5a) than that for the surface-based and EffB mean winds (65%).

For comparison purposes, the results for the 829 RUC cases (Fig. 5b) display similar patterns and distances between the curves relative to those for the 583 observed cases (Fig. 5a), but there also are some differences. First, the minimum MAE for the MU-based mean wind occurred at 55% of the height of the MUEL for the RUC dataset (Fig. 5b)—slightly less than the 60% for the observed dataset. This 5% decrease in optimal height for the RUC dataset also was noted for the surface-based and EffB mean winds. It is unknown if this lower top of the mean wind in the

---

[4] The results for the base of the height-based mean wind are quailtatively similar to those for the pressure-weighted mean wind (i.e., same MAE patterns and distances between curves). Thus, for brevity, we omitted discussion of these height-based results.

Figure 5. (a) MAE (m s^{-1}) of the forecast supercell motion for 583 observed cases where the base of the pressure-weighted mean wind was varied as follows: surface (blue); height of the MU parcel (red); and height of the effective inflow-layer base (EffB, black). The dashed gray horizontal line at 3.19 m s^{-1} indicates the minimum MAE for the 0–8-km pressure-weighted mean wind; this minimum was valid for all combinations (i.e., weightings, bases, depths, and tops) explored within the observed dataset. The top of the mean wind ranges from 30 to 80% of the height of the MUEL (roughly the storm top). (b) Same as (a) except for 829 RUC cases. The dashed gray horizontal line at 4.40 m s^{-1} indicates the minimum MAE for the 0–7-km pressure-weighted mean wind; this minimum was valid for all combinations (i.e., weightings, bases, depths, and tops) explored within the RUC dataset.

RUC dataset is truly representative of those supercell environments, or if instead this shallower layer is a function of the vertical grid spacing of the RUC from 1999 to 2005. Second, the minimum MAE for the MU-based mean wind in the RUC dataset is smaller than that for the surface-based and EffB mean winds, which is opposite that for the observed dataset. Third, the minimum MAE for the RUC dataset is 4.40 m s^{-1} (consistent with T07 who derived the dataset), which is 1.21 m s^{-1} greater than the MAE for the observed dataset herein. A systematic bias in the RUC model may have existed during that time, or perhaps there is

a systematic difference in the storm motion calculations between the observed and RUC datasets[5]. Nonetheless, all three methods have a minimum MAE that is nearly identical or up to 0.05 m s^{-1} larger than for the minimum for all combinations (cf. dashed line in Fig. 5b). Overall, the MU parcel was above the surface for 338 (40.8%) of the RUC cases, whereas the EffB was above the surface for only 51 (6.2%) of the cases. In addition, 40% of the EffB heights had a greater pressure than that of the MU parcel heights for the RUC dataset, but only two MU parcel heights had a greater pressure than that of the corresponding EffB.

For the observed dataset, all three methods have a minimum MAE that is 0.11–0.17 m s^{-1} larger than that for the minimum for all combinations (cf. dashed line in Fig. 5a). This finding suggests that the height of either the MU parcel or the EffB could be used in place of the surface for the base of the mean-wind calculation without detrimental effects, at least in a larger statistical sense. The effectiveness of the MU parcel and EffB as the base of the mean wind will be tested in the next section with the RUC dataset.

Finally, RD05 asserted that the supercell motion schemes are more sensitive to the mean-wind depth than the shear layer, and that is why the wind-shear layer was left unmodified in the abovementioned sensitivity tests for the mean wind. Nevertheless, for completeness the base and top of the wind-shear layer were allowed to vary according to the mean-wind bases and tops given in Fig. 5a (for the observed dataset). These results confirm that no improvement can be gained by allowing the wind-shear layer to deviate from the prescribed range given in B2K. In fact, the MAEs were slightly larger for nearly all layers tested. The results for modifying *only the base* of the shear layer also produced slightly larger MAEs.

e. Application of the RUC dataset to elevated, "shallow," and "tall" supercells

The observed results have been consulted to determine what bases and tops should be used for testing with the RUC dataset. This was done so as not to bias the results in favor of the RUC. In other words, we believe the observations should drive the testing. Therefore, the same mean-wind calculation layer can be tested with various model data, such as the RUC.

---

[5] There are 13 cases with overlap (i.e., same date, time, and sounding location) between the observed and RUC datasets. The MAEs for these small samples are 3.81 and 4.53 m s^{-1} for the observed and RUC, respectively.

Given that the results for the MU parcel height and the EffB were similar (section 3d), both methods were evaluated for their efficacy as the base of the mean wind. To test for elevated supercells, RUC cases were partitioned according to bases (MU and EffB) >750, 1000, 1250, 1500, and 2000 m AGL. Conversely, to test for "shallow" and "tall" supercells, RUC cases were partitioned by MUEL <7, 8, 9, and 10 km, as well as MUEL >14 km. Mean winds were calculated for pressure weighting [Eq. (2)] because (i) pressure weighting was shown to be superior to weighting by height and (ii) the additional computational costs are acceptable relative to the benefit of a broad range of fairly small MAEs. The top of the mean wind was set to 65% of MUEL based on the observed dataset. This mean wind was input into the supercell motion prediction using the B2K formulation, and the results were compared to the *default* B2K prediction (i.e., using a 0–6-km height-based mean wind).

As noted previously, for all cases there was virtually no difference in the MAEs for the default B2K method versus the two modifications using the pressure-weighted mean wind (Table 1, second column). However, for the elevated storm classifications the MU-based mean wind resulted in larger MAEs (0.12–0.48 m s^{-1})—relative to the default B2K method—for most partitions (Table 1, upper left). This finding may seem counterintuitive, but in cases where only modest surface-based CIN is present, a substantial fraction of surface-based air may be ingested by the storm updraft (Nowotarski et al. 2011), and thus contributes to the momentum of the storm. In these cases, the MU parcel height might be inappropriate in defining the inflow layer, even though the most buoyant air is above the EffB, and the ground.

Conversely, the EffB mean wind resulted in smaller MAEs for all partitions of elevated bases, with errors reduced by >1 m s^{-1} (Table 1, lower left). Moreover, as the EffB increased above the ground (and the supposed inflow layer also increased), the errors were reduced even further. One caveat, however, is that the sample sizes for the EffB elevated cases are much smaller than those for the MU-based elevated cases. Nevertheless, the EffB method appears to be filtering out the MU-based elevated cases that have marginal CIN, and thus behave more like surface-based supercells (Nowotarski et al. 2011; also see the example in section 3f). These results echo those of T07 stated in section 1, but a notable advantage is that the results here are independent of a priori knowledge of supercell type (i.e., surface-based versus elevated).

The results were somewhat reversed when considering variations in the MUEL heights (i.e., the MU-based method was better than the EffB method), but positive improvements still were yielded for the EffB method. For example, there was a 13–25% improvement in supercell motion predictions when the MUEL was <9 km AGL for the MU-based mean wind (Table 1, upper right). And these results improved as the MUEL decreased (but this decrease in MUEL also corresponds to a decrease in sample size). For the EffB mean wind (Table 1, lower right), the improvements were only 20–57% of those for the MU-based mean wind. Conversely, when the MUEL was >14 km AGL, the MAEs were larger than those for the default B2K method for both mean-wind options, especially for the MU-based mean wind (i.e., +0.59 m s^{-1}). Apparently the low-density air in the upper levels of very tall storms has little effect on storm motion, and thus no benefit can be gained by using a deeper mean-wind layer in these cases.

The supposed statistical significance (Nicholls 2001) of the difference in errors between the default B2K method and the B2K method using the two modified mean winds was assessed as described on p. 68 of B2K. In brief, the difference, d, was computed between the paired data, and the mean, $\bar{d}$, was examined to determine if it was significantly different from zero. Small p values [i.e., the probability of falsely rejecting the null hypothesis, Wilks (1995)] mean that the observed MAEs are unlikely to recur in two unrelated sets of data. Still, we cannot conclude that the MAEs are different between the two populations, and large p values do not mean that $\bar{d} = 0$ is highly probable (Ambaum 2010). The p values and percent-improvement statistics in Table 1 indicate that the most operationally relevant gains, on average, can be made for elevated storms, and secondarily for shallower supercells. The EffB method for the bottom of the mean wind produces consistently better results than the MU-based method.

f. Examples of supercell motion predictions for elevated and shallow supercells

Two brief examples are given in this section to illustrate the possible benefits of employing a modified mean wind for elevated (e.g., Calianese et al. 1996) and shallow (e.g., Clark 2009) supercells. Observed storm motions provided by these authors were used in the hodographs displayed below. In both cases the supercells were classified as high precipitation (Moller et

Table 1. Results for supercell motion predictions using the RUC dataset and variations to the pressure-weighted mean wind noted in section 3e (top of table is for MU-based, bottom of table is for EffB); variations were formulated based on the observed dataset. Cases were partitioned according to the height (AGL) of the MU parcel and EffB, as well as the MUEL. Blue bold-faced values (corresponding to negative MAE differences) represent improvements over the default B2K method and red bold-faced values (corresponding to positive MAE differences) represent worse predictions. MAE units are m s^{-1}. Refer to the text for a discussion of the *p* values.
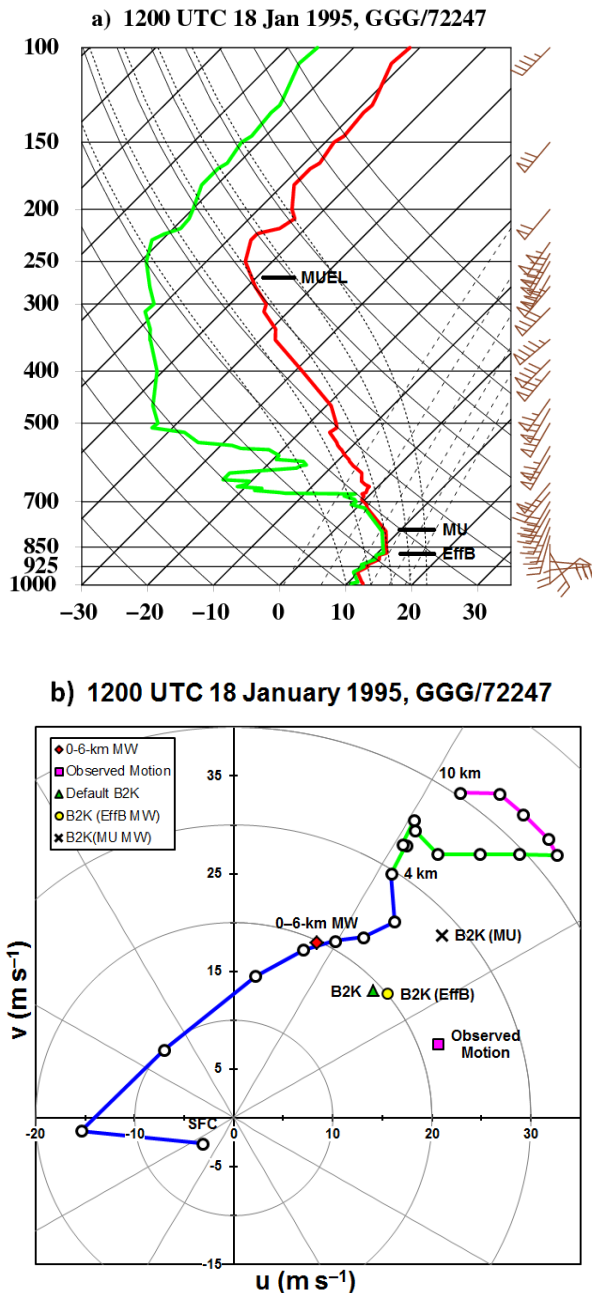
MU-based mean wind (pressure-weighted)										
Partitions	**All Cases**	**base >0.75 km**	**base >1 km**	**base >1.25 km**	**base >1.5 km**	**base >2 km**	**MUEL <7 km**	**MUEL <8 km**	**MUEL <9 km**	**MUEL <10 km**	**MUEL >14 km**
# cases	829	78	53	28	17	9	11	21	51	121	50
MAE for B2K	4.48	5.63	5.73	4.97	4.92	5.12	5.80	6.24	5.43	4.78	4.65
MAE for 65% MUEL	4.51	5.75	6.20	5.45	5.17	5.11	4.34	5.18	4.72	4.44	5.24
MAE diff. from B2K	+0.03	+0.12	+0.47	+0.48	+0.24	0.00	−1.46	−1.06	−0.71	−0.34	+0.59
MU % improvement	**−0.8%**	**−2.2%**	**−8.3%**	**−9.8%**	**−5.0%**	0.1%	**+25.1%**	**+17.1%**	**+13.2%**	**+7.1%**	**−12.7%**
p value	23.8%	36.3%	14.6%	25.4%	39.9%	49.9%	5.51%	2.66%	0.44%	0.65%	0.24%

EffB-based mean wind (pressure-weighted)										
Partitions	**All Cases**	**base >0.75 km**	**base >1 km**	**base >1.25 km**	**base >1.5 km**	**base >2 km**	**MUEL <7 km**	**MUEL <8 km**	**MUEL <9 km**	**MUEL <10 km**	**MUEL >14 km**
# cases	829	19	9	6	3	1	11	21	51	121	50
MAE for B2K	4.48	6.40	6.36	6.36	6.26	9.61	5.80	6.24	5.43	4.78	4.65
MAE for 65% MUEL	4.48	4.99	5.12	4.24	2.41	4.16	5.47	6.03	5.02	4.65	4.86
MAE diff. from B2K	0.00	−1.41	−1.24	−2.12	−3.85	−5.45	−0.33	−0.21	−0.41	−0.13	+0.21
EffB % improvement	**0.0%**	**+22.0%**	**+19.5%**	**+33.4%**	**+61.5%**	**+56.7%**	**+5.8%**	**+3.4%**	**+7.5%**	**+2.7%**	**−4.5%**
p value	48.0%	1.23%	10.1%	6.08%	3.77%	N/A	39.8%	38.7%	11.9%	20.3%	10.5%

al. 1994). The "modified" B2K methods below employ the pressure-weighted mean wind and 65% of the MUEL as the top of the mean wind.

The elevated supercell sounding from 18 January 1995 featured a MU parcel that was higher than the EffB (Fig. 6a), congruent with the results in section 3d.2. The sounding had zero surface-based CAPE and displayed a quasi-isothermal lapse rate in the boundary layer to near 850 hPa; thus, the supercell could be confidently classified as elevated. The EffB occurred at 1090 m AGL, resulting in CAPE and CIN of 543 and −10 J kg^{-1}, respectively. The MU parcel was 768 m higher than the EffB, possessing CAPE and CIN of 730 and −0.2 J kg^{-1}, respectively. Based on the work

of Nowotarski et al. (2011), the EffB appears to be a more realistic choice than the MU parcel for the inflow base in this scenario.

Predicted storm motions were in error by as much as 7.3–11.2 m s^{-1} (Fig. 6b); the storm deviated much farther off the hodograph than empirical methods would suggest. The largest error occurred for the modified B2K method using the MU parcel for the mean-wind base (black "X"); the smallest error occurred for the modified B2K method using the EffB for the mean-wind base (yellow circle)—1.2 m s^{-1} less than the error for the default B2K method (green triangle). The 768-m difference between the EffB and MU parcel height resulted in a storm motion error that was

a) **1200 UTC 18 Jan 1995, GGG/72247**

b) **1200 UTC 18 January 1995, GGG/72247**

Figure 6. (a) Observed skew$T$–log$p$ thermodynamic diagram for Longview, TX (GGG), valid 1200 UTC 18 January 1995. The relative heights of the EffB, MU parcel, and MUEL are indicated in black. The abscissa is temperature (°C) and the ordinate is pressure (hPa). The horizontal wind is given by half-barbs (2.6 m s^{-1} or 5 kt), full barbs (5.1 m s^{-1} or 10 kt), and/or pennants (25.7 m s^{-1} or 50 kt). (b) Observed 0–10-km hodograph valid the same time as in (a). Data and symbols are plotted every 500 m. The 0–6-km height-based mean wind is given by the red diamond; the observed supercell motion is given by the purple square; the default B2K supercell motion prediction is given by the green triangle; the modified B2K motion with the EffB mean wind is given by the yellow circle; and the modified B2K motion with the MU-parcel mean wind is given by the black "X" symbol. Calianese et al. (1996) has more details about this case.

3.9 m s^{-1} larger for the MU-based method, relative to the EffB. Too much of the lower atmosphere was discarded when using the MU parcel as the base of the mean wind. Thus, this case study illustrates (i) a modest improvement over the default B2K method when using the EffB-based mean wind for an elevated supercell and (ii) the drawback of using too high a base when computing the mean wind, which is more likely to occur with the MU parcel than with the EffB.
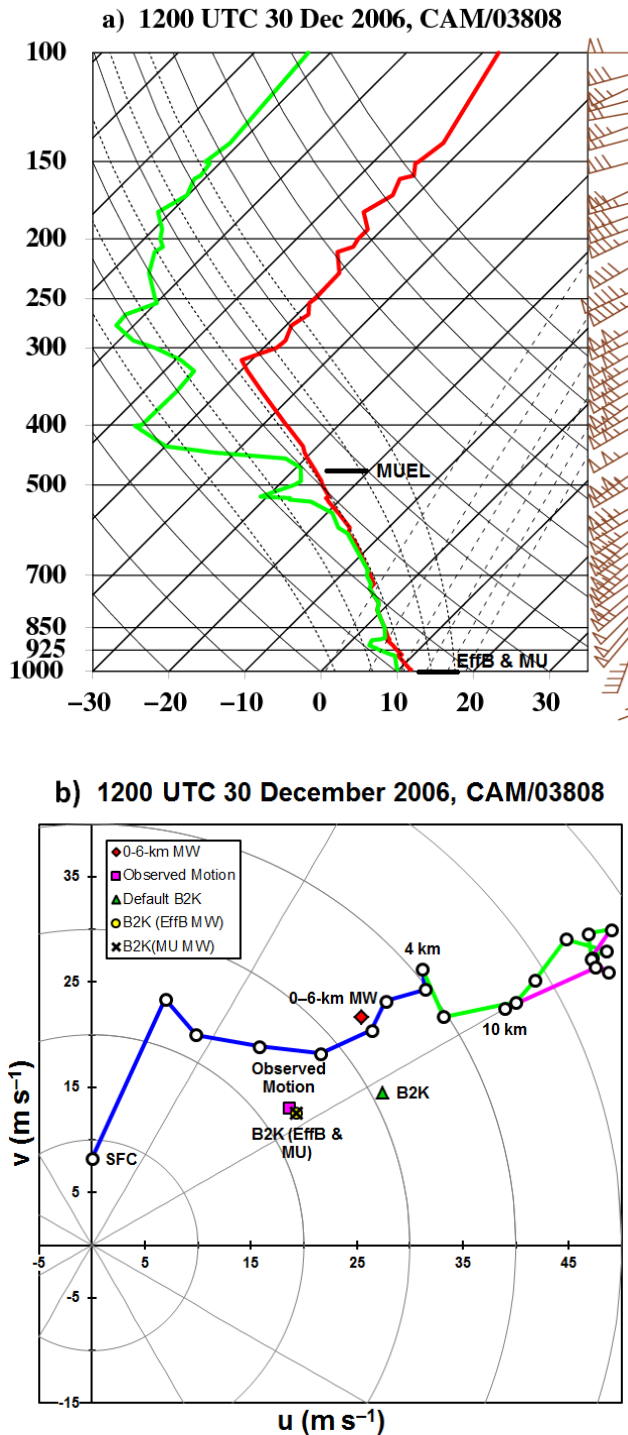
The sounding for the low-topped supercell from 30 December 2006 exhibited the same levels for the surface-based, MU-based, and EffB parcels (Fig. 7a), and hence there is no difference in the base of the mean wind among the varying methods. The CAPE was only 157 J kg^{-1} (with virtually no CIN), and the 0–6-km bulk wind difference was 49 m s^{-1}. This low-CAPE/high-shear environment is a relatively common scenario for these low-topped supercells (e.g., Vescio and Stuart 1994; Jungbluth 2002; Graham 2007; Richter 2007; Edwards et al. 2012). Given this environment, the MUEL was only 5676 m AGL—much lower than the typical 12 km (T07).

The default B2K method predicted a supercell motion that was 9.0 m s^{-1} faster than the observed storm motion (Fig. 7b). However, when using a mean wind that depends on the MUEL, the modified B2K method resulted in storm motion errors of only 0.9 m s^{-1} (i.e., the black "X," purple square, and yellow circle are nearly coincident in Fig. 7b). Although this is just a single case, it illustrates a potential problem when using an advection layer that is too deep for predicting the motion of low-topped supercells.

g. *The mean wind as a function of thermodynamic variables: Observed dataset*

As a final consideration, thermodynamic variables were compared to storm motion errors to address concerns raised by Kirkpatrick et al. (2007) that only kinematic information is used by the B2K method. This comparison was accomplished by correlating pertinent convective variables with three error metrics from the default B2K algorithm: (i) the *u*-component error; (ii) the error in the direction of the 0–6-km mean wind vector; and (3) the error in the direction of the 0–6-km shear vector. All three of these error types are strongly influenced by the mean wind, and also highly correlated with each other ($\rho > 0.80$).

The largest negative correlations were from –0.20 to –0.24 for the 700-hPa temperature and from –0.20 to –0.22 for the MLLCL. Correlations for the MLLFC

a) 1200 UTC 30 Dec 2006, CAM/03808

b) 1200 UTC 30 December 2006, CAM/03808

Figure 7. Same as Fig. 6 except for Camborne, England (CAM), valid 1200 UTC 30 December 2006. Clark (2009) has more details about this case.
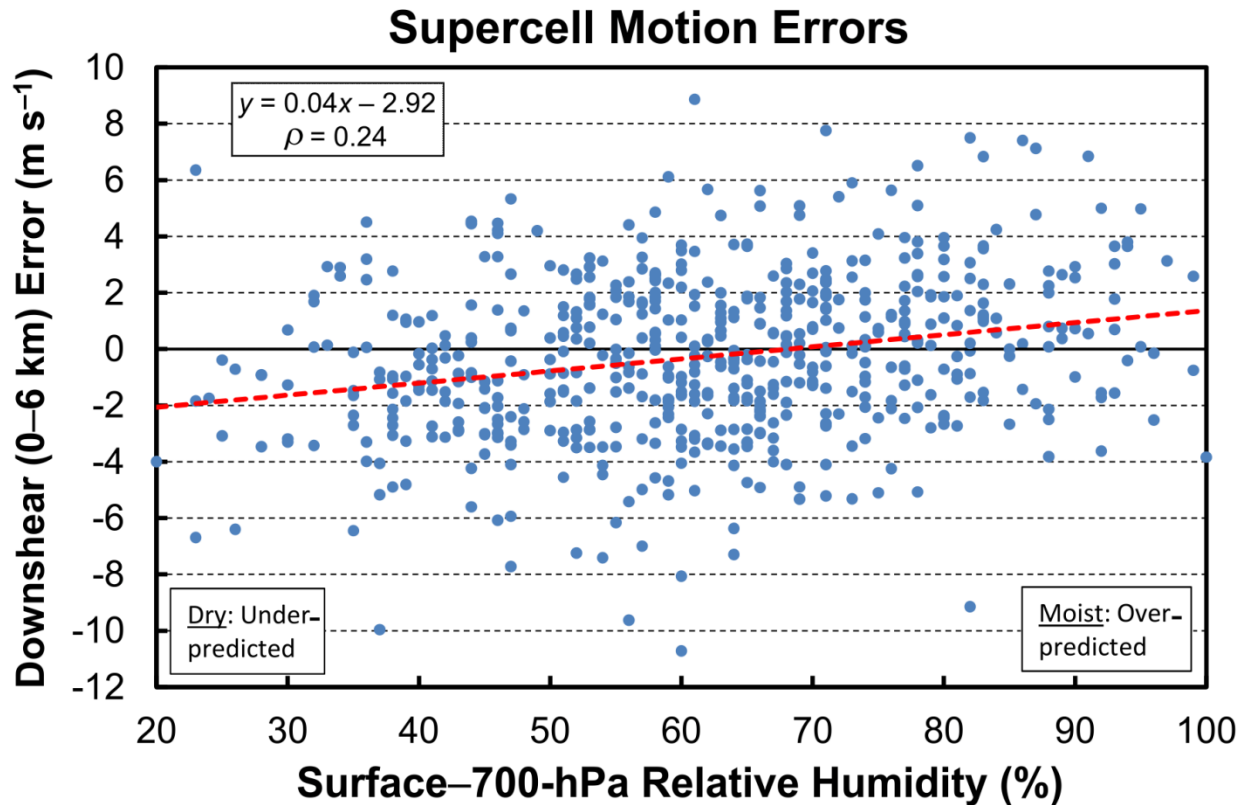
were from –0.11 to –0.14. Thus, relatively large 700-hPa temperatures and MLLCLs led to a tendency to *underpredict* supercell motion in the downwind/downshear direction (i.e., the motion error became

more negative, or less positive, as the 700-hPa temperatures and MLLCLs increased). Positive correlations occurred for the relative humidity in the surface–700-hPa layer (ρ = 0.21 to 0.24; Fig. 8). In this scenario, high relative humidity in the lower atmosphere was associated with a tendency to *overpredict* supercell motion in the downwind/downshear direction—perhaps indicative of a weak gust front. Even though the correlations are statistically significant, the results are meteorologically insignificant. Specifically, the supercell motion MAE increased by 0.11 m s^{-1} when setting the mean wind as a function of the surface–700-hPa relative humidity (i.e., using the regression equation in Fig. 8). Finally, the lowest correlations ($|\rho|$ <0.05) occurred for MLCAPE, MLEL, and 0–1-km AGL mixing ratios.

4. Conclusion

At least one possibility appears tenable for calculating a universal mean wind when used in supercell motion forecasts: *pressure-weighted, using the EffB height as the base, and 65% of the height of the MUEL as the top*. This method works as well as the default B2K method for all cases using both the observed and RUC datasets, and, furthermore, succeeds for elevated supercells—something that is not necessarily true of the 0–6-km height-based mean wind. Rasmussen and Blanchard's (1998) method (among others) also conceivably could be adjusted for this alternative mean wind. Although results are less robust for relatively shallow supercells, a MUEL-based top for the mean wind may be useful in these situations, as implied by a case study. This latter speculation can be tested further when a larger observational dataset of these kinds of supercells becomes available. Additional testing is important considering the bias toward typical supercell cases across the central United States in both the observed and RUC datasets.

The current work also reinforces previous findings that a pressure-weighted mean wind over a relatively deep layer of the atmosphere is generally superior to a height-based mean wind. The differences are modest, but may justify use. The pressure-weighted mean wind also is more consistent with the contribution of horizontal momentum to thunderstorm motion (e.g., Hitschfeld 1960; Newton 1960). Regarding the height-based mean wind, the present study disagrees with RD05's claim that 0–8 km is better than 0–6 km for the mean-wind layer used in the B2K method. An examination of height- and pressure-weighting schemes,

Figure 8. Scatterplot of surface–700-hPa relative humidity (%) versus the default B2K supercell motion error (m s^{-1}) in the downshear (0–6 km) direction for 580 observed supercell cases. MUCAPE was required to be ≥50 J kg^{-1}. The red dashed line is the linear regression of the data. This correlation ($\rho = 0.24$) was the highest for the thermodynamic variables tested. Positive errors represent cases where the forecast supercell motion was faster than the observed motion (in the downshear direction).

and their application to observed and RUC datasets, suggests that the 0–8-km layer is suboptimal for the height-based mean wind. Therefore, forecasters are advised to be cognizant of the mean wind used in operations.

To conclude, null and/or insignificant results can be useful in illuminating dead-end paths that future research can avoid (Schultz 2009, p. 42)—at least with similar methods and datasets. Although we propose a modification to the mean-wind calculation for the B2K method, these results do reaffirm that the 0–6-km height-based mean wind is reasonably robust, with little gained by more complicated methods. At the same time, proper anticipation of the mean wind in elevated and low-topped supercell environments *may help* with forecaster situational awareness for potentially high-impact severe weather.

REFERENCES

Ambaum, M. H. P., 2010: Significance tests in climate science. *J. Climate,* **23,** 5927–5932, CrossRef.

Atkins, N. T., M. L. Weisman, and L. J. Wicker, 1999: The influence of preexisting boundaries on supercell evolution. *Mon. Wea. Rev.*, **127**, 2910–2927, CrossRef.

Bunkers, M. J., 2002: Vertical wind shear associated with left-moving supercells. *Wea. Forecasting*, **17**, 845–855, CrossRef.

____, 2006: An observational assessment of off-hodograph deviations for use in operational supercell motion forecasting methods. Preprints, *23rd Conf. on Severe Local Storms*, St. Louis, MO, Amer. Meteor. Soc., 8.6. [Available online at ams.confex.com/ams/pdfpapers/115414.pdf.]

____, and J. W. Zeitler, 2000: On the nature of highly deviant supercell motion. Preprints, *20th Conf. on Severe Local Storms*, Orlando, FL, Amer. Meteor. Soc., 236–239.

____, B. A. Klimowski, J. W. Zeitler, R. L. Thompson, and M. L. Weisman, 2000: Predicting supercell motion using a new hodograph technique. *Wea. Forecasting*, **15**, 61–79, CrossRef.

____, M. R. Hjelmfelt, and P. L. Smith, 2006: An observational examination of long-lived supercells. Part I: Characteristics, evolution, and demise. *Wea. Forecasting*, **21**, 673–688, CrossRef.

Calianese, E. J., Jr., A. R. Moller, and E. B. Curran, 1996: A WSR-88D analysis of a cool season, elevated high-precipitation supercell. Preprints, *18th Conf. on Severe Local Storms*, San Francisco, CA, Amer. Meteor. Soc., 96–100.

Chappell, C. F., 1986: Quasi-stationary convective events. *Mesoscale Meteorology and Forecasting*, P. S. Ray, Ed., Amer. Meteor. Soc., 289–310.

Cintineo, R. M., and D. J. Stensrud, 2013: On the predictability of supercell thunderstorm evolution. *J. Atmos. Sci.*, **70**, 1993–2011, CrossRef.

Clark, M. R, 2009: The southern England tornadoes of 30 December 2006: Case study of a tornadic storm in a low CAPE, high shear environment. *Atmos. Res.*, **93**, 50–65, CrossRef.

Corfidi, S. F., S. J. Corfidi, and D. M. Schultz, 2008: Elevated convection and castellanus: Ambiguities, significance, and questions. *Wea. Forecasting,* **23,** 1280–1303, CrossRef.

Darbe, D., and J. Medlin, 2005: Multi-scale analysis of the 13 October 2001 central Gulf Coast shallow supercell tornado outbreak. *Electronic J. Operational Meteor.,* **6** (1), 1–7. [Available online at www.nwas.org/ej/pdf/2005-EJ1.pdf.]

Davies, J., 1990: Midget supercell spawns tornadoes. *Weatherwise*, **43**, 260–261, CrossRef.

____, 1993: Small tornadic supercells in the central plains. Preprints, *17th Conf. on Severe Local Storms*, St. Louis, MO, Amer. Meteor. Soc., 305–309. [Available online at www.jondavies.net/1993_SLS_mini-sprcl/1993_SLS_mini-sprcl.htm.]

____, and R. H. Johns, 1993: Some wind and instability parameters associated with strong and violent tornadoes. 1. Wind shear and helicity. *The Tornado: Its Structure, Dynamics, Prediction, and Hazards, Geophys. Monogr.*, No. 79, Amer. Geophys. Union, 573–582, CrossRef.

Doswell, C. A., III, and E. N. Rasmussen, 1994: The effect of neglecting the virtual temperature correction on CAPE calculations. *Wea. Forecasting*, **9**, 625–629, CrossRef.

Edwards, R., A. R. Dean, R. L. Thompson, and B. T. Smith, 2012: Convective modes for significant severe thunderstorms in the contiguous United States. Part III: Tropical cyclone tornadoes. *Wea. Forecasting*, **27**, 1507–1519, CrossRef.

Graham, R., 2007: 21 May 2001: Environmental and radar aspects of a significant low-topped supercell tornado outbreak across southern lower Michigan. *Natl. Wea. Dig.*, **31**, 36–46. [Available online at nwas.org/digest/papers/2007/Vol31-Issue1-Jul2007/Pg36-Graham.pdf]

Grant, B. N., 1995: Elevated cold-sector severe thunderstorms: A preliminary study. *Natl. Wea. Dig.,* **19** (4), 25–31. [Available online at nwas.org/digest/papers/1995/Vol19-Issue4-Jul1995/Pg25-Grant.pdf]

____, and R. Prentice, 1996: Mesocyclone characteristics of mini supercell thunderstorms. Preprints, *15th Conf. on Weather Analysis and Forecasting,* Norfolk, VA, Amer. Meteor. Soc., 362–365.

Hitschfeld, W., 1960: The motion and erosion of convective storms in severe vertical wind shear. *J. Meteor.*, **17**, 270–282, CrossRef.

Jungbluth, K., 2002: The tornado warning process during a fast-moving low-topped event: 11 April 2001 in Iowa. Preprints, *21st Conf. on Severe Local Storms*, San Antonio, TX, Amer. Meteor. Soc., 329–332. [Available online at ams.confex.com/ams/pdfpapers/46917.pdf.]

Kirkpatrick, J. C., E. W. McCaul Jr., and C. Cohen, 2007: The motion of simulated convective storms as a function of basic environmental parameters. *Mon. Wea. Rev.,* **135,** 3033–3051, CrossRef.

Maddox, R. A., 1976: An evaluation of tornado proximity wind and stability data. *Mon. Wea. Rev.*, **104**, 133–142, CrossRef.

McCaul, E. W., Jr., and M. L. Weisman, 1996: Simulations of shallow supercell storms in landfalling hurricane environments. *Mon. Wea. Rev.*, **124**, 408–429, CrossRef.

Moller, A. R., C. A. Doswell III, M. P. Foster, and G. R. Woodall, 1994: The operational recognition of supercell thunderstorm environments and storm structures. *Wea. Forecasting*, **9**, 327–347, CrossRef.

Newton, C. W., 1960: Morphology of thunderstorms and hailstorms as affected by vertical wind shear. *Physics of Precipitation, Geophys. Monogr.*, No 5, Amer. Geophys. Union, 339–347.

____, and J. C. Fankhauser, 1964: On the movements of convective storms, with emphasis on size discrimination in relation to water-budget requirements. *J. Appl. Meteor.*, **3**, 651–668, CrossRef.

Nicholls, N., 2001: The insignificance of significance testing. *Bull. Amer. Meteor. Soc.*, **82**, 981–986, CrossRef.

Nowotarski, C. J., P. M. Markowski, and Y. P. Richardson, 2011: The characteristics of numerically simulated supercell storms situated over statically stable boundary layers. *Mon. Wea. Rev.*, **139**, 3139–3162, CrossRef.

Ramsay, H. A., and C. A. Doswell III, 2005: A sensitivity study of hodograph-based methods for estimating supercell motion. *Wea. Forecasting,* **20,** 954–970, CrossRef.

Rao, G. V., J. W. Scheck, R. Edwards, and J. T. Schaefer, 2005: Structures of mesocirculations producing tornadoes associated with tropical cyclone Frances (1998). *Pure Appl. Geophys.*, **162**, 1627–1641, CrossRef.

Rasmussen, E. N., and D. O. Blanchard, 1998: A baseline climatology of sounding-derived supercell and tornado forecast parameters. *Wea. Forecasting*, **13**, 1148–1164, CrossRef.

Richter, H., 2007: A cool-season low-topped supercell tornado event near Sydney, Australia. Preprints, *33rd Int. Conf. on Radar Meteorology,* Cairns, Australia, Amer. Meteor. Soc., P13A.16. [Available online at ams.confex.com/ams/pdfpapers/123550.pdf.]

Schultz, D. M., 2009: *Eloquent Science: A Practical Guide to Becoming a Better Writer, Speaker, and Atmospheric Scientist*. Amer. Meteor. Soc., 412 pp, CrossRef.

Spratt, S. M., D. W. Sharp, P. Welsh, A. Sandrik, F. Alsheimer, and C. Paxton, 1997: A WSR-88D assessment of tropical cyclone outer rainband tornadoes. *Wea. Forecasting,* **12,** 479–501, CrossRef.

Thompson, R. L., R. Edwards, J. A. Hart, K. L. Elmore, and P. Markowski, 2003: Close proximity soundings within supercell environments obtained from the Rapid Update Cycle. *Wea. Forecasting*, **18**, 1243–1261, CrossRef.

____, C. M. Mead, and R. Edwards, 2007: Effective storm-relative helicity and bulk shear in supercell thunderstorm environments. *Wea. Forecasting,* **22,** 102–115, CrossRef.

Vescio, M. D., and N. A. Stuart, 1994: Synoptic and mesoscale features leading to the 10 March 1992 Charlotte, North Carolina tornado: A low-top, weak-reflectivity, severe weather event. *Natl. Wea. Dig.*, **18** (4), 29–42. [Available online at nwas.org/digest/papers/1994/Vol18-Issue4-Jun1994/Pg29-Vescio.pdf]

Weaver, J. F., 1979: Storm motion as related to boundary-layer convergence. *Mon. Wea. Rev.*, **107**, 612–619, CrossRef.

Weisman, M. L., and J. B. Klemp, 1986: Characteristics of isolated convective storms. *Mesoscale Meteorology and Forecasting,* P. S. Ray, Ed., Amer. Meteor. Soc., 331–358.

Wicker, L. J., and L. Cantrell, 1996: The role of vertical buoyancy distributions in miniature supercells. Preprints*, 18th Conf. on Severe Local Storms*, San Francisco, CA, Amer. Meteor. Soc., 225–229.

Wilks, D. S., 1995: *Statistical Methods in the Atmospheric Sciences*. Academic Press, 467 pp.

Wilson, J. W., and D. L. Megenhardt, 1997: Thunderstorm initiation, organization, and lifetime associated with Florida boundary layer convergence lines. *Mon. Wea. Rev.*, **125**, 1507–1525, CrossRef.

Zeitler, J. W., and M. J. Bunkers, 2005: Operational forecasting of supercell motion: Review and case studies using multiple datasets. *Natl. Wea. Dig.*, **29**, 81–97. [Available online at nwas.org/digest/papers/2005/Vol29No1/Pg81-Zeitler.pdf.]